Danny Chan

Optical investigations of bioorganic systems by spectrally resolved ellipsometry

Cuvillier Verlag Göttingen

Universität Hamburg

Fachbereich Physik

Optical investigations of bioorganic systems by spectrally resolved ellipsometry

Dissertation

zur Erlangung des Doktorgrades
des Fachbereichs Physik
der Universität Hamburg

vorgelegt von
Danny Chan
aus Hamburg

Hamburg, 2005

Bibliografische Information Der Deutschen Bibliothek
Die Deutsche Bibliothek verzeichnet diese Publikation in der Deutschen Nationalbibliografie; detaillierte bibliografische Daten sind im Internet über http://dnb.ddb.de abrufbar.
1. Aufl. - Göttingen : Cuvillier, 2005
Zugl.: Hamburg, Univ., Diss., 2005
ISBN 3-86537-505-7

Gutachter der Dissertation:	Prof. Dr. M. Rübhausen Prof. Dr. U. Hahn
Gutachter der Disputation:	Prof. Dr. M. Rübhausen Dr. R. Wepf
Datum der Disputation:	26.05.2005
Vorsitzender des Prüfungsausschusses:	Dr. K. Petermann
Vorsitzender des Pomotionsausschusses:	Prof. Dr. G. Huber
Dekanin / Dekan des Fachbereichs:	Prof. Dr. G. Huber

© CUVILLIER VERLAG, Göttingen 2005
Nonnenstieg 8, 37075 Göttingen
Telefon: 0551-54724-0
Telefax: 0551-54724-21
www.cuvillier.de

Alle Rechte vorbehalten. Ohne ausdrückliche Genehmigung des Verlages ist es nicht gestattet, das Buch oder Teile daraus auf fotomechanischem Weg (Fotokopie, Mikrokopie) zu vervielfältigen.
1. Auflage, 2005
Gedruckt auf säurefreiem Papier

ISBN 3-86537-505-7

Inhaltsangabe

Methoden für quantitative Spektroskopie an biologischer Geweben basieren häufig auf der Analyse des diffus gestreuten Lichts [1, 2]. Im Gegensatz dazu wird in dieser Arbeit die spektral aufgelöste Ellipsometrie für biophysikalische Anwendungen diskutiert. Die Ellipsometrie misst die Änderung der Polarisation von Licht bei der direkten Reflexion an einer Probenoberfläche. Diese Technik hat mehrere interessante Eigenschaften, wie z.B. Selbstnormalisierung, niedrige Energiedichten im Strahl und Empfindlichkeit auf morphologische und chemische Parameter über den komplexen Brechungsindex. Die hohe Informationsdichte der Messungen erfordern jedoch eine nicht-triviale, numerisch aufwendige Auswertung.

In Wissenschaft und Industrie wird die Ellipsometrie zumeist für die Charakterisierung von Festkörpersystemen mit kontrollierten und gut strukturierten Eigenschaften eingesetzt. Die bei biologischen Systemen deutlich erhöhte Komplexität der Morphologie der Systeme ist sicherlich mit ein Grund für die geringe Anzahl an wissenschaftlichen Publikationen in diesem Feld. Als Beispiele für Veröffentlichungen in diesem Bereich seien hier Untersuchung von Insektenflügeln und Muskelfasern genannt, sowie Messungen der Hydrationsdynamik menschlicher Nägel [3–5].

Die biologischen Systeme in dieser Arbeit sind zumeist Haut und Hautanhänge wie Haare und Nägel. Die Bedeutung dieser Gewebe für landgebundenes Leben sollte nicht unterschätzt werden. Im Laufe dieser Arbeit wurden hierbei Messungen der Hydrationsdynamik menschlicher Nägel gemacht, welche zeigen, dass Ellipsometrie zwischen gebundenem und freien Wasser unterscheiden kann. Eine im weiteren durchgeführte “Tapestripping”-Studie zeigt, dass die Technik detaillierte Profile der optischen und strukturellen Parameter der menschlichen Haut liefern kann. Die zu Ende der Arbeit gezeigten Resultate von menschlichen Haaren schließlich betonen die Empfindlichkeit der Technik für Oberflächeneffekte. Die dabei gezeigte Differenzierung zwischen Proben mit unterschiedlichen, typischen Produktbehandlungen demonstrieren, dass Ellipsometrie eine für industrielle Applikationen interessante Technik darstellt.

Zuletzt zeigen erste Messungen an den Wurzeln von *allium cepa*, der gewöhnlichen Küchenzwiebel, dass dieses System ein geeignetes Modellsystem darstellt, um ein tieferes Verständnis für die Ausbreitung von polarisiertem Licht in biologischen Geweben zu erlangen, insbesondere in Hinblick auf den Einfluss des experimentellen Setups selber.

Die Zusammenfassung der gesammelten Erfahrungen führt schließlich auf eine Liste von instrumentellen Eigenschaften, welche von einem für biologische Applikationen optimierten Ellipsometer erfüllt werden sollten.

Introduction

Methods for quantitative tissue spectroscopy are often based on the analysis of diffusively scattered light [1, 2]. This work in contrast discusses the application of spectrally resolved ellipsometry to biophysical problems. Optical ellipsometry is a technique that measures the change in polarization of a light beam due to direct reflection on a sample surface. It has several interesting properties, such as self normalization, low power densities in the probe beam and sensitivity to both morphological as well as chemical parameters. The high information density of ellipsometric spectra however comes with the price of a non-trivial analysis.

Ellipsometry is used in the scientific community and in industrial applications for the characterization of solid state systems, where the samples under investigation are typically well controlled and well structured, thereby reducing the complexity of the analysis considerably. This is a likely reason for the lack of ellipsometric applications for bioorganic systems in the literature. Publications employing ellipsometry for biological systems include investigations of the structure of insect wings and muscle fibers, as well as measurements of the hydration dynamics of human nails [3–5].

The biological systems investigated in this work are mainly skin and skin appendages such as hairs and nails. The importance of these systems for terrestrial live cannot be overemphasized. In the course of this work, measurements of the hydration dynamics of human nails were performed, that show the ability of ellipsometric techniques to distinguish between bound and free water in a bioorganic sample. A tapestripping study on human skin reveals the depth profile of structural parameters of the skin and shows, that ellipsometry is able to resolve fine details in the optical and structural parameters. Finally, measurements on human hair show the sensitivity of ellipsometry to surface roughness effects in biological media. The ability of ellipsometry to resolve the effects of typical products on the hair emphasizes, that this technique can become a useful technique for industrial applications.

Somewhat unrelated biologically are measurements on *allium cepa*, the normal onion. The preliminary results of these measurements show however, that this system can be used as a simple model system to gain a deeper understanding of the interaction of polarized light in biological tissues, especially with regard to the influence of the instrumental setup.

The experience gained in the course of this work leads finally to a characterization of the most beneficial properties of ellipsometry for biological applications and a listing of instrumental properties for a specialized bio-ellipsometer.

Contents

Contents **7**

List of Figures **9**

1 Theory and Instrumental Details **13**
1.1 Principle of Ellipsometry . . . 13
1.1.1 Maxwell Equations . . . 14
1.1.2 Mathematical Representation of Polarization . . . 15
1.1.3 Jones Vector and Jones Matrix Formalism . . . 16
1.1.4 Photometric Ellipsometry . . . 17
1.2 Modelling Ellipsometric Spectra . . . 18
1.2.1 Reflection on a Bulk System - the Fresnel Coefficients . . . 18
1.2.2 Layered systems . . . 20
1.2.2.1 Ambient/Film/Substrate system . . . 20
1.2.2.2 Stratified planar isotropic systems . . . 21
1.2.3 Effective Medium Approximation . . . 23
1.3 Numerical Optimization . . . 24
1.3.1 L-BFGS-B . . . 25
1.3.2 Differential Evolution . . . 26
1.3.3 Simulated Annealing . . . 28
1.4 Instrumental Details . . . 30

2 Investigated Biological Systems: Skin and Skin Appendages **33**
2.1 Nail . . . 33
2.2 Skin . . . 35
2.3 Hair . . . 37

3 Experiments **41**
3.1 Studies on Allium Cepa . . . 41
3.2 Hydration Studies on Human Fingernails . . . 43
P I Hydration dynamics of human fingernails: An ellipsometric study . 56
P II Spectroscopic ellipsometry on biological materials — investigation of hydration dynamics and structural properties . . . 61

3.3 In-Vivo Study on Human Skin 61
P III In-vivo spectroscopic ellipsometry measurements on human skin . . 75
3.4 Structural Studies on Human Hair 75
3.4.1 Single Hair Measurements 75
3.4.2 Measurements on Hair Strands 76
3.4.3 A Dielectric Model of the Hair 85
P IV Structural investigations of human hairs by spectrally resolved ellipsometry 103

4 Summary **103**

5 Conclusions and Outlook **105**

Bibliography **109**

Acknowledgements **113**

A A Programmer's Overview over ElliPy2 **115**

List of Figures

1.1 Schematic setup of an ellipsometer. R_p, R_s: complex reflection coefficients for parallel and perpendicular component, respectively; α_1, α_2: angle of the polarizer and analyzer; ϕ_0: angle of incidence. 13

1.2 Parameters determining the Polarization Ellipse: Azimuth angle Θ, amplitude A and ellipticity $\tan\epsilon = b/a$. The time dependence of the electric field vector can be described by superposition of two linearly, along the coordinate axis polarized orthogonal waves $E_x(\vec{r},t)$ and $E_y(\vec{r},t)$. 16

1.3 Interference in an ambient/film/substrate system 21

1.4 Influence of interface roughnesses on the polarization; a) The optical path length of the partial waves is changed by the height modulation of the interface roughness; b) The interface roughness is modelled by an additional layer with an effective complex refractive index given by an effective medium comprised of the two media. 24

2.1 Schematic picture of the human fingernail; PNF: proximal nail fold, NM: nail matrix, CU: cuticle, L: lunula, NB: nail bed, NP: nail plate, HYP: hyponchium 34

2.2 Schematic overview of skin 35

2.3 Microscopic picture of the epidermis, showing the sublayers in various stages of differentiation 36

2.4 Schematic representation of the hair follicle, showing the inner root sheat (IRS) and the outer root sheath (ORS). 38

2.5 Schematic picture of a hair fibre 38

3.1 Ψ spectrum of an onion root, measured at several positions along the root. Bold line: Ψ spectrum of a silicon wafer 42

3.2 Comparison of the behaviour of the refractive index in a nail hydration/dehydration experiment and the dehydration of a piece of bovine liver. a) Changes in the refractive index of a human nail clipping on hydration; both the absolute value and the shape of the spectrum are changing; b) Comparison of wavelength averages of the refractive index of a nail hydration experiment and the dehydration of liver; full lines are results of a fit of eq. 3.1 44

3.3 Long time hydration dynamics of nails. a) Volume content profile of the free and bound water states; b) development of the refractive index n and absorption coefficient k in a long time hydration/dehydration experiment; full and dashed line are the result of the model shown schematically in figure 3.4 45
3.4 Model of the hydration dynamics of nails. Free water is incorporated into the nail matrix (large circles) and then converted to bound water (small circles). On dehydration evaporation of free water occurs as well as further conversion to bound water. 47
3.5 Setup for tapestrip measurements 61
3.6 Comparison of a tapestrip experiment on human skin (left column) and the hydration of a human nail clipping (right column). The parameters show similar effects in both experiments, indicating an similar mechanism. . . . 62
3.7 Model of the human skin for modelling the tapestrip experiments. Cells and lipid layers are modelled by isotropic layer matrices according to eq. 1.23. D_R, f_{Air}: thickness and air inclusion of the roughness layer; f_{H2O}: water volume ratio in the cell; D_C: thickness of the cell; D_L, f_L: thickness and cell medium inclusion in the lipid layer; d: distance into the skin. 63
3.8 Result of the fit of the model depicted in figure 3.7 for one representative measurement. Full line: measured spectrum; dashed line: calculated spectrum 65
3.9 Results obtained by a fit in a tapestrip experiment. a) assumed water inclusion profile f_{H2O}; b) air inclusion f_{Air} in the roughness layer; c) lipid inclusion f_L in the lipid layer; d) thickness of the roughness layer D_R; e) thickness of the cell layer D_C; f) thickness of the lipid layer D_L 65
3.10 Sample holder for single hair measurements consisting of pieces of sandblasted silicon 76
3.11 Single hair measurements on 10 positions along an european natural blond hair. Left: hair oriented parallel to the plane of incidence; right: hair oriented perpendicular to the plane of incidence. Values of Δ in the range $180° \leq \Delta \leq 360°$ are mapped to the range $-180° - 0°$ for better visibility of the zero crossings in the parallel orientation. 77
3.12 Setup for measurements on hair strands. The hairs are fixated in a bridge configuration to prevent back reflexes from the sample holder 78
3.13 Measurements of Ψ and Δ on strands of human hair from single persons. Left column: measurements on darker hair types; right column: measurements on brighter hair types. For each person, two samples were measured, marked by equal color and the circles. 79
3.14 Ψ-Δ spectra for two samples with different angle of incidence ϕ_0. Left: european blond hair; right: european black hair. The upper insets are the refractive index in the same wavelength range with an y-axis scaling from 1.38 to 1.48. The lower insets are the absorption coefficient k in the same wavelength range with an y-axis scaling from 0 to 0.15. The complex refractive indices were computed assuming the bulk model from eq. 1.17 . 79

3.15 Ψ-Δ spectra of european natural blond hairs, damaged by different exposure to artificial sunlight. 80
3.16 Ψ-Δ spectra of hairs treated with two hair sprays. Left column: european natural blond hair; right column: bleached blond hair. The reference spectrum is the average of ten samples prior to product application. The spectra labeled "product 1"and "product 2" are each averages of the spectra of five treated samples. Error bars give the standard deviation over all measurements. 81
3.17 Ψ-Δ spectra of undamaged, european natural blond hairs treated by two different shampoos. Dashed line indicates height of the Δ spectrum in the region 400 to 600 nm, while arrows estimate the slope of the curve. For each treatment, three samples are shown. Error bars give the standard deviation of the measurements on different positions on one sample. 83
3.18 Ψ-Δ spectra of damaged, bleached european natural blond hairs treated by two different shampoos. Dashed lines indicate height and position of the peak in the Δ spectrum in the region 400 to 600 nm. For each treatment, three samples are shown. Error bars give the standard deviation of the measurements on different positions on one sample. 84
3.19 Schematic representation of the dielectric layer model for human hair. d_{ACu}: thickness interface air/cuticle; f_A: effective medium ratio cuticle/air; d_{Cu}: thickness cuticle; n_{Cu}, k_{Cu}: refractive index and absorption coefficient of the cuticle; d_{CuCo}: thickness interface cuticle/cortex; f_{CuCo}: effective medium ratio cortex/cuticle; n_{Co}, k_{Co}: refractive index and absorption coefficient of the cortex. 85
3.20 Measured and calculated spectra in a multi-angle fit with $\phi_0 = 63°, 65°$, and $70°$. Full lines: measured spectra; dashed lines: calculated spectra given by the model shown in figure 3.19 while assuming constant dispersions for the cuticle and the cortex. a) european black; b) european brown; c) european natural blond; d) chinese; e) european blond; f) european red. 87
3.21 Ψ-Δ spectra calculated from the model of figure 3.19 using two different values for the thickness of the cuticle. Full line: $d_{Cu} = 1.72\,\mu$m; dashed line: $d_{Cu} = 1\,\mu$m 88
3.22 Structural and optical parameters of the cuticle surface layer calculated by fits to Ψ-Δ measurements on human hair strands. 1: european black, 2: european brown, 3: european natural blond, 4: chinese, 5: european blond, 6: european red. Column 5 and 6 belong to hairs showing a peak structure in the parameter Δ. The most prominent differences to the other samples are marked by bold typeface 88
3.23 Measured and calculated spectra in a multi-angle fit with $\phi_0 = 63°, 65°$, and $70°$. Full lines: measured spectra; dashed lines: calculated spectra given by the model shown in figure 3.19. Left column: european black hair; right column: european blond hair. The model was first assuming constant dispersions as for figure 3.20, followed by a pointwise fit of the cuticle and cortex dispersion while holding the structural parameters fixed. 89

3.24 Optical parameters of the cuticle and cortex of an european natural black hair. Left column: refractive index and absorption coefficient of the cuticle; right column: refractive index and absorption coefficient of the cortex. The optical parameters were obtained by a fit of the model while assuming constant dispersions, followed by fitting the dispersions wavelength dependent while keeping the structural parameters fixed. 90
3.25 Δ spectrum caused by changing structural and optical parameters of the cuticle/air interface. a) Change in the thickness of the roughness layer; b) change in the air content of the roughness layer; c) change in the absorption coefficient k of the cuticle. 92

Chapter 1

Theory and Instrumental Details

1.1 Principle of Ellipsometry

The measurements described in this thesis were made using spectrally resolved ellipsometry. While the basic experimental setup of an ellipsometer is relatively simple, the interpretation of the measured spectra is not trivial.

In ellipsometry, the change in polarization of a light beam upon reflection on a sample is measured. The basic setup of an ellipsometer is shown in figure 1.1. A light beam from a white light source or a monochromatic source such as a laser is polarized and incident on the sample under an angle ϕ_0 with the surface normal. The directly reflected light from the sample surface is analyzed using a second polarizer. The resulting intensity in dependence on the analyzer angle is then detected at the detector.

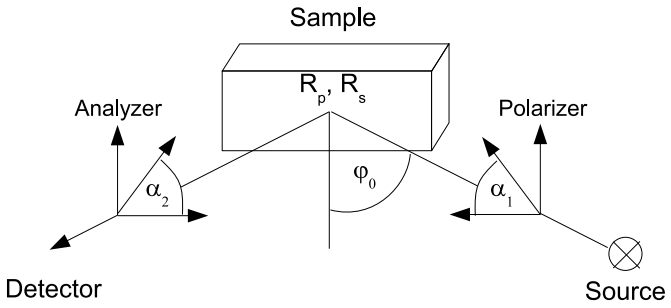

Figure 1.1: Schematic setup of an ellipsometer. R_p, R_s: complex reflection coefficients for parallel and perpendicular component, respectively; α_1, α_2: angle of the polarizer and analyzer; ϕ_0: angle of incidence.

The polarization change is quantified in terms of the ellipsometric parameters Ψ and Δ. These parameters are related to the sample properties by

$$\tan\Psi\, e^{i\Delta} = \frac{R_p}{R_s} \quad , \tag{1.1}$$